Journal of Virology

Virology | Full-Length Text

Nuclear proinflammatory cytokine S100A9 enhances expression of human papillomavirus oncogenes via transcription factor TEAD1

Seiichiro Mori,[1] Yoshiyuki Ishii,[1] Takamasa Takeuchi,[1] Iwao Kukimoto[1]

AUTHOR AFFILIATION See affiliation list on p. 17.

ABSTRACT Transcription of the human papillomavirus (HPV) oncogenes, *E6* and *E7*, is regulated by the long control region (LCR) of the viral genome. Although various transcription factors have been reported to bind to the LCR, little is known about the transcriptional cofactors that modulate HPV oncogene expression in association with these transcription factors. Here, we performed *in vitro* DNA-pulldown purification of nuclear proteins in cervical cancer cells, followed by proteomic analyses to identify transcriptional cofactors that bind to the HPV16 LCR via the transcription factor TEAD1. We detected the proinflammatory cytokine S100A9 that localized to the nucleus of cervical cancer cells and associated with the LCR via direct interaction with TEAD1. Nuclear S100A9 levels and its association with the LCR were increased in cervical cancer cells by treatment with a proinflammatory phorbol ester. Knockdown of S100A9 decreased HPV oncogene expression and reduced the growth of cervical cancer cells and their susceptibility to cisplatin, whereas forced nuclear expression of S100A9 using nuclear localization signals exerted opposite effects. Thus, we conclude that nuclear S100A9 binds to the HPV LCR via TEAD1 and enhances viral oncogene expression by acting as a transcriptional coactivator.

IMPORTANCE Human papillomavirus (HPV) infection is the primary cause of cervical cancer, and the viral oncogenes *E6* and *E7* play crucial roles in carcinogenesis. Although cervical inflammation contributes to the development of cervical cancer, the molecular mechanisms underlying the role of these inflammatory responses in HPV carcinogenesis are not fully understood. Our study shows that S100A9, a proinflammatory cytokine, is induced in the nucleus of cervical cancer cells by inflammatory stimuli, and it enhances HPV oncogene expression by acting as a transcriptional coactivator of TEAD1. These findings provide new molecular insights into the relationship between inflammation and viral carcinogenesis.

KEYWORDS HPV, viral oncogenes, TEAD1, S100A9, transcriptional coactivator, proinflammatory cytokine

Human papillomaviruses (HPVs) are a family of small viruses with a circular double-stranded DNA genome of approximately 8,000 bp (1, 2). HPV infects basal cells of stratified epithelia and undergoes replication along with the differentiation of infected cells (1). More than 200 HPV genotypes have been identified, including the high-risk types HPV16 and HPV18, which cause cervical, vulvar, vaginal, anal, penile, and oropharyngeal cancers (1). The genomes of the high-risk types often get integrated into host chromosomes during persistent infection, resulting in aberrant expression of the viral oncoproteins, E6 and E7, which inactivate p53 and Rb, respectively, thereby inhibiting apoptosis and promoting cell cycle progression (1, 2). Constantly elevated E6 and E7

Editor Lawrence Banks, International Centre for Genetic Engineering and Biotechnology, Trieste, Italy

Address correspondence to Seiichiro Mori, moris@niid.go.jp.

The authors declare no conflict of interest.

See the funding table on p. 18.

Received 30 May 2023
Accepted 20 June 2023
Published 14 August 2023

levels immortalize and transform cervical epithelial cells, leading to the development of invasive cervical cancer. Although persistent infection with high-risk HPVs is the primary cause of cervical carcinogenesis, inflammation induced by genital infection with HPV or other pathogenic viruses, bacteria, and fungi contributes to the development of HPV-induced cervical cancer (3–7).

Expression of the viral early genes for E6 and E7 is regulated by a non-coding region of approximately 750 bp, called the long control region (LCR), located upstream of the *E6* gene (8, 9). The central part of the LCR contains enhancer elements that drive the transcription of early genes from the early promoter (P97 for HPV16 and P105 for HPV18) in an epithelial cell-specific manner (8–10). Various transcription factors (TFs) bind to and activate these enhancer elements, including AP-1, NFI, and TEAD1 (8–14). The LCR is often retained in chromosomally integrated HPV genomes and regulates viral oncogene expression (15). Thus, it is important to elucidate the regulatory mechanisms of LCR-driven transcription to gain insights into the molecular basis of HPV carcinogenesis.

Eukaryotic transcriptional complexes are composed of multiple proteins, including TFs and cofactors that regulate gene expression by binding to TFs. We previously identified 11 TEAD1-binding sites in the HPV16 LCR enhancer region and showed that the transcriptional cofactor VGLL1 binds to the HPV LCR via TEAD1 (16). Depletion of VGLL1 and/or TEAD1 decreased viral oncogene expression, whereas overexpression of VGLL1 or TEAD1 alone was insufficient to enhance transcription (14, 16). VGLL1 and TEAD1 have no transcriptional activity of their own (17, 18), suggesting the existence of additional cofactors that regulate HPV gene expression via TEAD1.

S100A9 is a small (14 kDa) multifunctional protein secreted by myeloid and epithelial cells, including keratinocytes (19–21). S100A9 forms a heterodimer with S100A8 and acts as a proinflammatory cytokine through toll-like receptor 4 (TLR4) and the receptor for advanced glycation end products, which, in turn, activates the NF-κB and AP-1 pathways (19–23). S100A9 regulates leukocyte chemotaxis and tissue infiltration in mice and exerts antimicrobial effects by sequestering zinc and manganese required for bacterial growth (21, 22, 24). Moreover, S100A9 has intracellular functions in the cytoplasm, functioning as a calcium sensor and regulating cytoskeleton rearrangement, arachidonic acid metabolism, and resistance to bacterial invasion (20, 21), thus playing a protective role in the innate immune response. Recent studies have reported that S100A9 nuclear localized where it regulates cellular gene transcription in association with genomic regulatory regions (25–27). Furthermore, S100A9 expression is elevated during various biological processes, such as inflammation, infection, wound healing, cell differentiation, and carcinogenesis (19–21).

In this study, we aimed to identify the transcriptional cofactors that regulate HPV oncogene expression via TEAD1. We performed *in vitro* DNA-pulldown followed by proteomic analyses to detect protein complexes on the HPV16 LCR. We observed that nuclear S100A9 transactivates HPV oncogene expression via TEAD1, contrary to its protective role in microbial infections.

RESULTS

Identification of TEAD1-interacting cofactors that bind to the HPV16 LCR

To identify transcriptional cofactors bound to the LCR via TEAD1, we performed *in vitro* DNA-pulldown assays followed by data-independent acquisition mass spectrometry (DIA-MS), which enables qualitative and quantitative proteomic analyses (28). We prepared a biotinylated DNA probe spanning nucleotides 7,623–7,760 of the HPV16 genome (wild-type [WT] LCR probe), harboring five previously identified TEAD1-binding sites (T7–T11) (14, 16) (Fig. 1A). We also prepared an LCR probe with mutations in the TEAD1-binding sites (Mut LCR probe) to distinguish TEAD1-interacting cofactors from other proteins that bind to the LCR independently of TEAD1 (Fig. 1A). We incubated the WT and Mut LCR probes with nuclear extracts from CaSki cells, a cervical cancer cell line with integrated HPV16 genomes (Fig. 1B). After affinity purification with streptavidin

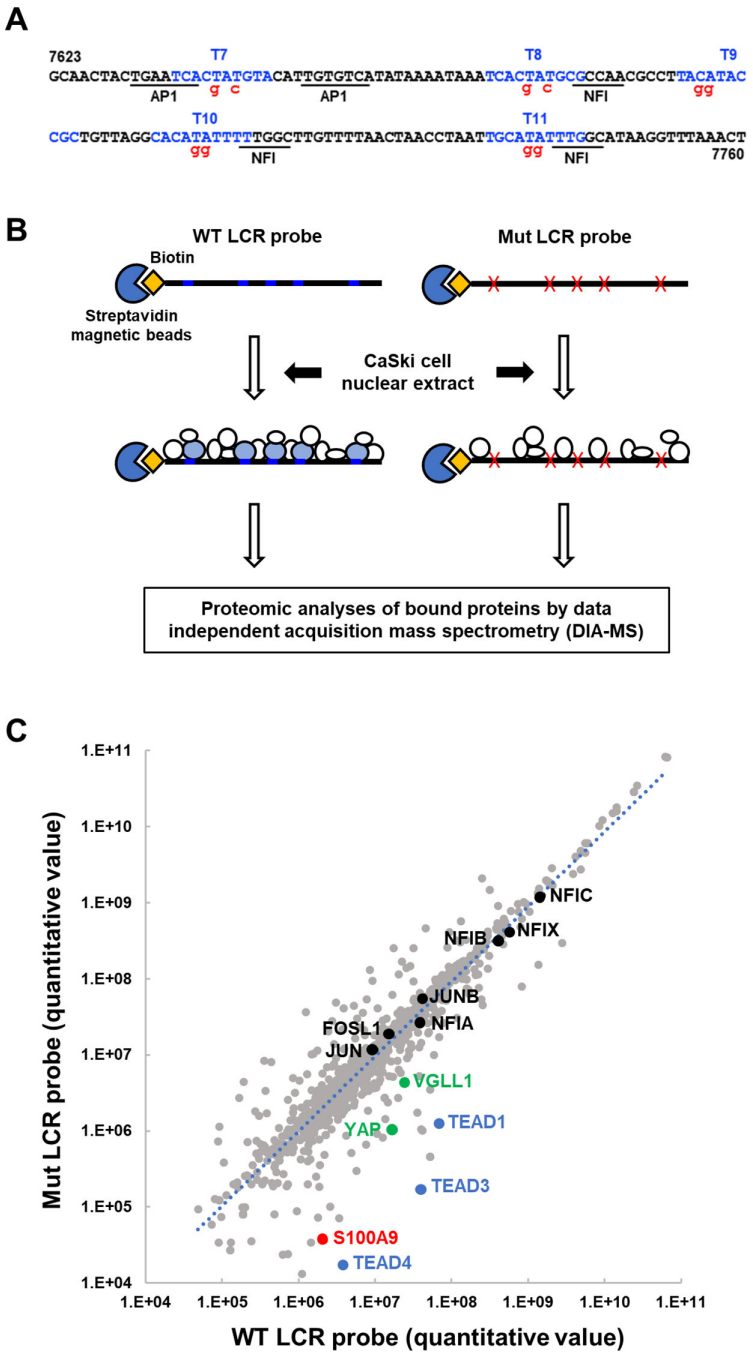

FIG 1 Identification of TEAD1-interacting cofactors that bind to the HPV16 LCR. (A) Nucleotide sequences of the WT and Mut LCR probes. Previously identified TEAD-binding sequences (T7–T11) (14, 16) are indicated in blue, and the nucleotide sequences of the Mut LCR probe are denoted in red. The binding motifs for NFI and AP-1 are underlined. (B) A schematic workflow for the identification of TEAD1-interacting cofactors. Biotinylated WT or Mut LCR probes coupled to Dynabeads/M-280 streptavidin were incubated with the nuclear extract of CaSki cells. Bound proteins were affinity purified and analyzed by data-independent acquisition mass spectrometry analyses. (C) The quantitative values of the identified proteins bound to the WT and Mut LCR probes are plotted on the *x*- and *y*-axes, respectively. The TEAD family of transcription factors is indicated in blue, and known TEAD-interacting cofactors are indicated in green. The S100A9 protein is indicated in red, and the NFI and AP-1 transcription factors are indicated in black. Other proteins are indicated by gray dots.

beads, we analyzed the bound proteins by DIA-MS and identified more than 1,000 proteins, including TEAD1, that preferentially bound to the WT LCR probe (Fig. 1C). As expected, TEAD3 and TEAD4 were also identified, but our previous study has shown that these TEADs are not primarily involved in HPV16 gene expression (16). We listed up a total of 39 proteins, including TEAD1, with a fivefold or greater reduced binding to the Mut LCR probe compared with that of the WT probe (Table 1). Notably, these 39 proteins included the well-known TEAD1-interacting cofactors YAP and VGLL1, indicating that this strategy is successful in the identification of proteins that bind to the LCR via TEAD1. Although four TEAD1-binding sequences (T7, T9, T10, and T11) partially overlapped with the binding motifs for NFI and AP-1 (Fig. 1A), the Mut LCR probe retained the binding sequences for these TFs, preserving their binding to the LCR (Fig. 1C). We detected about 60-fold reduced binding of S100A9 to the Mut LCR probe and investigated it further because it was recently reported to be involved in cellular gene transcription (25–27).

Nuclear expression of S100A9 in cervical cancer cells

The nuclear functions of S100A9 have been reported in keratinocytes (25), myeloid cells (26), and breast epithelial cells (27) but not in cervical cancer cells. We first confirmed nuclear localization of S100A9 in cervical cancer cell lines using immunofluorescence staining. We detected S100A9 in the cytoplasm and punctate nuclear staining in CaSki cells (Fig. 2A) and HeLa cells (an HPV18-positive cervical cancer cell line) (Fig. 2B) by confocal immunofluorescence microscopy. Furthermore, the Human Protein Atlas database (29) showed S100A9 in the nuclei of malignant cells from cervical cancer tissues (https://www.proteinatlas.org/ENSG00000163220-S100A9/pathology/cervical+cancer).

S100A9 expression is induced by a proinflammatory phorbol ester, 12-O-tetradecanoylphorbol-13-acetate (TPA), in keratinocytes (25). We confirmed whether TPA induces the expression of S100A9 in cervical cancer cells. We treated serum-starved CaSki cells with TPA or dimethyl sulfoxide (DMSO) for 4 h and determined S100A9 levels by cell fraction and immunoblotting. We observed increased S100A9 levels in both the cytoplasm and the nucleus after TPA treatment (Fig. 2C). S100A9 was detected in the insoluble nuclear fraction, along with histone H3, as reported for mouse keratinocytes (25). The inflammatory TF c-Fos was also upregulated in TPA-treated cells, confirming that TPA induced inflammatory responses. Thus, S100A9 is present in the nuclei of cervical cancer cells, and its expression is induced by inflammatory stimuli.

S100A9 associates with the HPV LCRs via direct binding to TEAD1

To determine whether S100A9 binds directly or indirectly to the LCR, we performed *in vitro* DNA-pulldown assays with hemagglutinin (HA)-tagged S100A9 (S100A9-HA) and FLAG-tagged TEAD1 (FLAG-TEAD1) that were purified from HEK293FT cells transfected with expression plasmids for S100A9-HA (pCMV-A9) and FLAG-TEAD1 (pCMV-FLAG-TEAD1), respectively (Fig. 3A). We did not detect direct binding between S100A9-HA and the WT LCR probe (Fig. 3B), whereas FLAG-TEAD1 clearly showed binding to it (Fig. 3C). However, when mixed with FLAG-TEAD1, S100A9-HA was found to bind to the WT LCR probe but not to the Mut LCR probe (Fig. 3D). These results suggest that S100A9 indirectly binds to the LCR via TEAD1.

To evaluate whether S100A9 interacts with TEAD1 in cells, we performed co-immunoprecipitation (Co-IP) experiments using nuclear extracts from CaSki cells and found that endogenous TEAD1 co-precipitated with S100A9 by anti-S100A9 antibodies (Fig. 3E). S100A9 also co-precipitated TEAD4, but the efficiency of the interaction was lower than that with TEAD1, consistent with our previous finding that TEAD4 knockdown in CaSki cells had little effect on HPV16 gene expression (16). Notably, one of the TEAD1-interacting cofactors, VGLL1, which is required for HPV gene expression (16), was also co-precipitated, suggesting that S100A9 forms a complex with VGLL1/TEAD1. In contrast, nuclear-abundant Ku70 was not co-precipitated, indicating the specificity of the interaction between S100A9 and TEAD1. S100A9 interacted with TEAD1 in nuclear extracts from HaCaT cells (HPV-negative, immortalized human skin keratinocytes) and

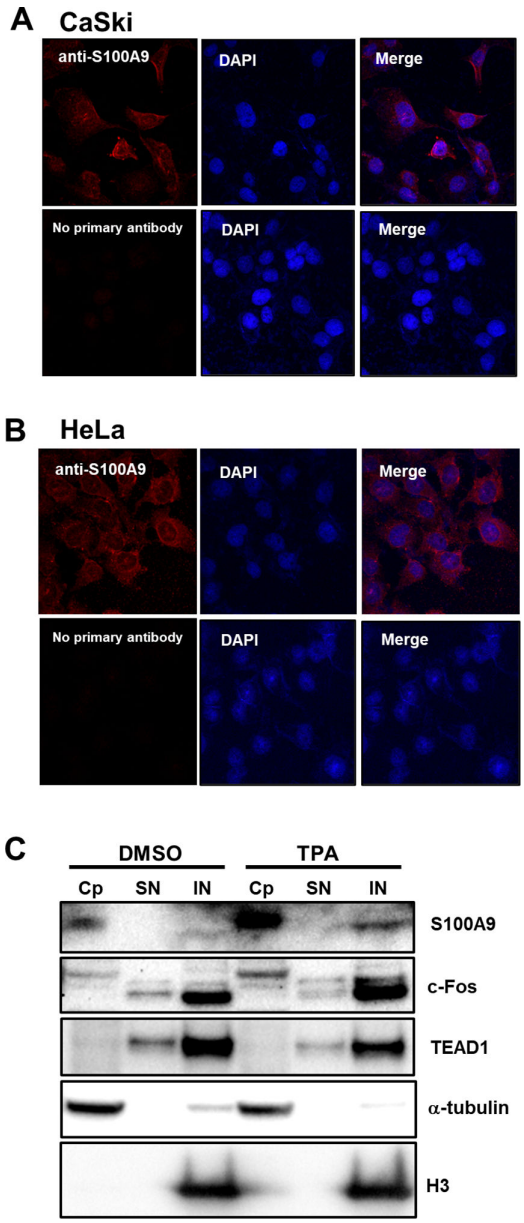

FIG 2 Nuclear expression of S100A9 in cervical cancer cells. (A and B) Immunofluorescence staining of S100A9 (red) in CaSki (A) and HeLa (B) cells. Cells were fixed and incubated with an anti-S100A9 monoclonal antibody, followed by an incubation with Alexa Fluor 546-conjugated secondary antibody (upper panels) or with the secondary antibody alone (lower panels). The nuclei were stained with DAPI (blue), and the cells were examined with a confocal microscope. (C) Cytoplasmic (Cp), soluble nuclear (SN), and insoluble nuclear (IN) fractions of CaSki cells treated with 200 ng/mL of 12-O-tetradecanoylphorbol-13-acetate (TPA) or dimethyl sulfoxide (DMSO) alone for 4 h after serum starvation were analyzed by immunoblotting with anti-S100A9, anti-c-Fos, and anti-TEAD1 antibodies, respectively. α-Tubulin and histone H3 (H3) were used as markers for the cytoplasmic and insoluble nuclear fractions, respectively.

HCK1T cells (HPV-negative, immortalized human cervical keratinocytes) (30), with lower efficiency than in CaSki cells (Fig. 3F and G), suggesting that the S100A9/TEAD1 interaction is enhanced in HPV-positive cancer cells. Therefore, endogenous S100A9 interacts with TEAD1 in both HPV-positive and HPV-negative cells.

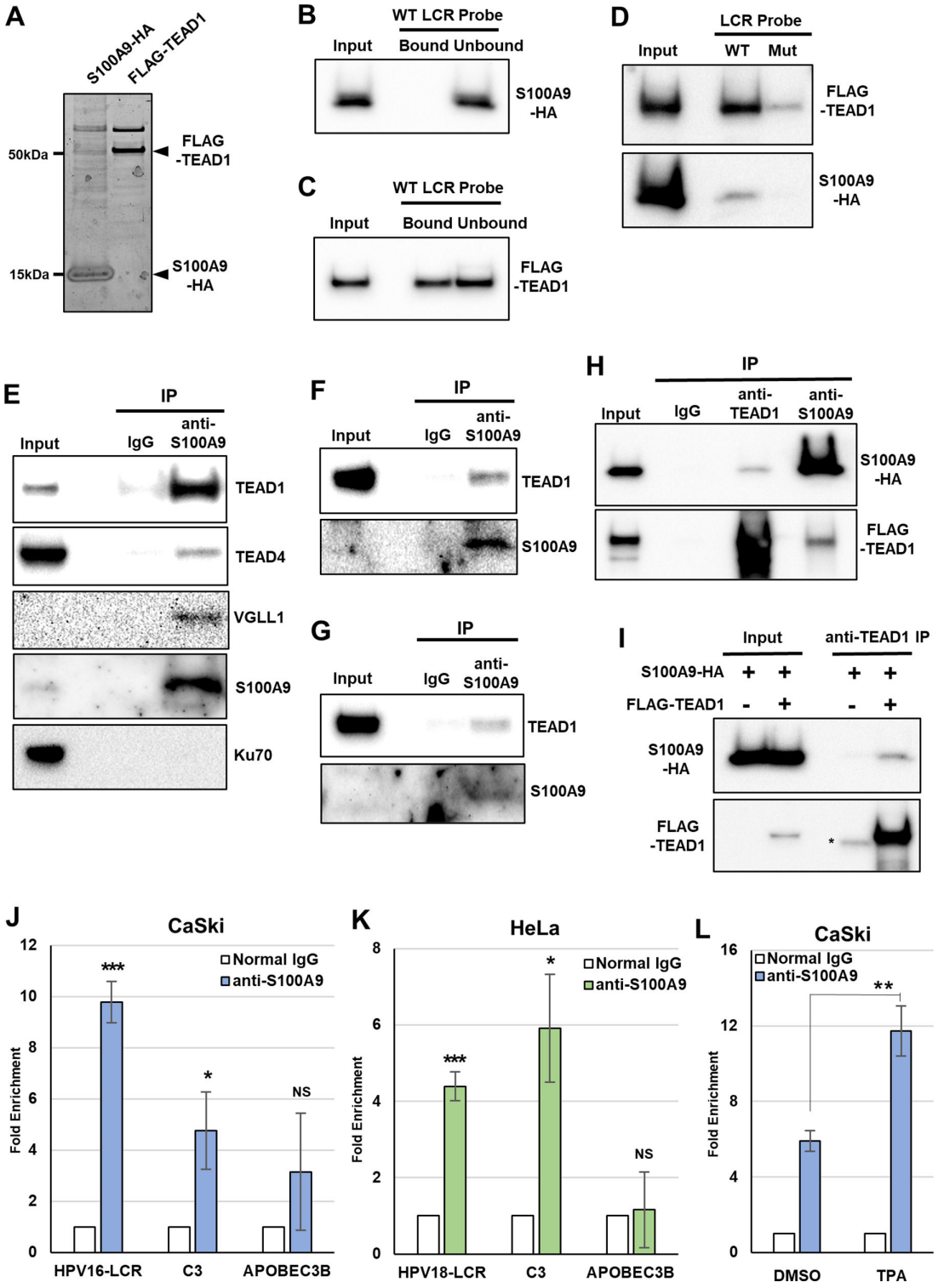

FIG 3 S100A9 associates with the HPV LCR via direct binding to TEAD1. (A) Sypro Ruby-stained polyacrylamide gel of purified proteins from HEK293 cells transfected with the expression plasmid for S100A9-HA or FLAG-TEAD1 (arrowhead). (B–D) The WT or Mut LCR probes were coupled to Dynabeads/M-280 streptavidin and incubated with the purified recombinant S100A9-HA (B), FLAG-TEAD1 (C), or the mixture of both proteins (D). Twenty percent of the input volume (Input), the unbound fraction (Unbound), and the total precipitated fraction (Bound) were analyzed by immunoblotting with anti-HA (B, D) or anti-FLAG (C, D) antibodies. (E-G) The nuclear extract isolated from CaSki (E), HaCaT (F), or HCK1T (G) cells was incubated with normal rabbit IgG or anti-S100A9 antibodies. One percent of the input volume (Input) and the total precipitated fractions (IP) were analyzed by immunoblotting with anti-TEAD1, anti-TEAD4, anti-VGLL1,

(Continued on next page)

FIG 3 (Continued)

anti-S100A9, and anti-Ku70 antibodies. (H) The mixture of the *in vitro*-translated S100A9-HA and FLAG-TEAD1 proteins was incubated with normal rabbit IgG, anti-TEAD1, or anti-S100A9 antibodies. Two percent of the input volume (Input) and the total precipitated fractions (IP) were analyzed by immunoblotting with anti-HA and anti-TEAD1 antibodies. (I) The *in vitro*-translated S100A9-HA protein alone or together with the FLAG-TEAD1 protein was incubated with anti-TEAD1 antibodies. Two percent of the input volume (Input) and the total precipitated fractions (anti-TEAD1 IP) were analyzed by immunoblotting with anti-HA and anti-FLAG antibodies. The asterisk indicates the heavy chains of the anti-TEAD1 antibodies used for immunoprecipitation. (J–L) Cross-linked chromatin prepared from CaSki (J), HeLa (K), or serum-starved CaSki cells treated with TPA or DMSO alone (L) was immunoprecipitated using anti-S100A9 antibodies or normal rabbit IgG, and the recovered DNA was quantified using real-time PCR with primers for the HPV16 (J, L) and HPV18 (K) LCRs. The promoter regions of the complement component 3 (*C3*) and *APOBEC3B* genes were amplified as positive and negative controls, respectively. The levels of S100A9 binding to the HPV16 or HPV18 LCR are shown as fold enrichment of the LCR DNA with anti-S100A9 antibodies relative to that with normal IgG. The data are averages from three experiments performed using independent chromatin preparations, with the error bars representing standard deviations. NS, $P > 0.05$; *, $P < 0.05$; **, $P < 0.01$; ***, $P < 0.005$ (Student's *t* test).

We then tested whether S100A9 directly binds to TEAD1 by performing Co-IP experiments using *in vitro*-translated proteins. We found that anti-TEAD1 antibodies co-precipitated S100A9-HA, and reciprocally, anti-S100A9 antibodies co-precipitated FLAG-TEAD1 (Fig. 3H). Anti-TEAD1 antibodies failed to recover S100A9-HA when FLAG-TEAD1 was excluded (Fig. 3I). We used an *in vitro* translation system with minimal *Escherichia coli* proteins (31), suggesting that S100A9 directly binds to TEAD1. The efficiency of co-precipitation of *in vitro*-translated FLAG-TEAD1 with S100A9-HA was lower than that of endogenous TEAD1 with S100A9 (Fig. 3E), suggesting that post-translational modifications of S100A9 and TEAD1 and/or association with other nuclear protein(s) may enhance the interaction. Taken together, these results demonstrate that S100A9 associates with the HPV LCR via a direct interaction with TEAD1.

We performed chromatin immunoprecipitation (ChIP) to determine whether nuclear S100A9 is associated with the LCR in cervical cancer cells. We utilized a two-step cross-linking method to detect indirect associations of transcriptional cofactors with DNA (see Materials and Methods). We found that S100A9 bound to the HPV16 LCR in CaSki cells (Fig. 3J) and the HPV18 LCR in HeLa cells (Fig. 3K). The complement component 3 (*C3*) gene, known to be associated with S100A9 in keratinocytes (25), was also bound by S100A9 in cervical cancer cells. In contrast, S100A9 binding to the promoter region of the *APOBEC3B* gene, which is regulated by TEADs (32), was not statistically significant, suggesting that not all TEAD-regulated genes are associated with S100A9. Next, we examined whether TPA treatment enhances S100A9 association with the LCR. We found that serum starvation reduced the association of S100A9 with the LCR compared to that in cells cultured in medium containing 10% fetal bovine serum (FBS) (compare Fig. 3J with 3L) and that TPA treatment restored this association (Fig. 3L). Thus, endogenous S100A9 is associated with the HPV LCR in cervical cancer cells, and inflammatory stimuli enhance the association.

S100A9 contributes to HPV oncogene expression

To examine whether S100A9 plays a role in HPV early gene expression, we transfected siRNA against S100A9 (siS100A9) into CaSki or HeLa cells, and quantified the levels of *E6*I* mRNA, a spliced isoform of the E6 transcripts expressed from the viral early promoter (33), by reverse transcriptase quantitative PCR (RT-qPCR). We observed a significant reduction in *E6*I* mRNA levels after S100A9 knockdown in both cell lines (Fig. 4A and B), with greater reduction in CaSki cells compared to that in HeLa cells, which correlated with the levels of S100A9 bound to the LCR (Fig. 3J and K). As we have previously reported (16), transfection of siRNA against TEAD1 (siTEAD1) into these cells significantly reduced *E6*I* mRNA levels (Fig. 4A and B). Combined knockdown of S100A9 and TEAD1 did not further decrease *E6*I* mRNA levels compared to that by individual S100A9 or TEAD1 knockdown (Fig. 4A and B), suggesting that S100A9 and TEAD1 act together to regulate HPV oncogene expression. S100A9 also enhanced HPV oncogene expression in non-tumor cells; S100A9 knockdown in W12 cells (HPV16-positive, human cervical

TABLE 1 Proteins with a fivefold or greater reduced binding to the Mut LCR probe compared with that of the WT probe

UniProt accession number	Protein name	Gene name	WT LCR probe[a]	Mut LCR probe[a]	Fold decrease (WT/Mut)
Q99594	Transcriptional enhancer factor TEF-5	TEAD3	4.1.E+07	1.7.E+05	240.3
Q15561	Transcriptional enhancer factor TEF-3	TEAD4	3.8.E+06	1.7.E+04	223.8
P07477	Trypsin-1	PRSS1	5.3.E+07	4.7.E+05	112.8
P05089	Arginase-1	ARG1	1.1.E+06	1.3.E+04	83.9
P06702	Protein S100A9	S100A9	2.1.E+06	3.7.E+04	57.9
P28347	Transcriptional enhancer factor TEF-1	TEAD1	7.0.E+07	1.3.E+06	55.7
P05109	Protein S100A8	S100A8	3.4.E+06	7.1.E+04	48.4
P20930	Filaggrin	FLG	1.4.E+06	3.4.E+04	42.0
P81605	Dermcidin	DCD	4.2.E+07	1.0.E+06	40.9
P02538	Keratin, type II cytoskeletal 6A	KRT6A	4.0.E+07	1.1.E+06	37.5
Q96P63	Serpin B12	SERPINB12	7.2.E+05	2.4.E+04	29.5
Q13835	Plakophilin-1	PKP1	6.2.E+05	2.4.E+04	25.9
Q5D862	Filaggrin-2	FLG2	2.6.E+06	1.0.E+05	25.5
Q9NUP9	Protein lin-7 homolog C	LIN7C	1.8.E+06	7.3.E+04	24.6
P02533	Keratin, type I cytoskeletal 14	KRT14	3.5.E+07	1.8.E+06	20.1
Q02413	Desmoglein-1	DSG1	5.6.E+06	3.0.E+05	18.7
P46937	Transcriptional coactivator YAP1	YAP1	1.8.E+07	1.0.E+06	17.1
Q5T749	Keratinocyte proline-rich protein	KPRP	1.2.E+07	8.3.E+05	15.0
Q8IY63	Angiomotin-like protein 1	AMOTL1	5.2.E+07	3.5.E+06	14.8
Q9UIF9	Bromodomain adjacent to zinc finger domain protein 2A	BAZ2A	7.6.E+06	6.7.E+05	11.4
Q86YZ3	Hornerin	HRNR	1.1.E+07	9.3.E+05	11.3
P31944	Caspase-14	CASP14	9.5.E+05	8.9.E+04	10.7
P13645	Keratin, type I cytoskeletal 10	KRT10	8.3.E+08	7.9.E+07	10.4
Q8NI35	InaD-like protein	PATJ	1.8.E+06	1.9.E+05	9.8
Q96BR9	Zinc finger and BTB domain-containing protein 8A	ZBTB8A	4.9.E+06	5.2.E+05	9.4
P04264	Keratin, type II cytoskeletal 1	KRT1	2.8.E+09	3.0.E+08	9.4
P08779	Keratin, type I cytoskeletal 16	KRT16	1.3.E+07	1.4.E+06	9.3
P35527	Keratin, type I cytoskeletal 9	KRT9	1.3.E+09	1.5.E+08	8.8
P62633	Cellular nucleic acid-binding protein	CNBP	2.0.E+07	2.8.E+06	7.2
Q53EQ6	Tigger transposable element-derived protein 5	TIGD5	3.7.E+07	5.3.E+06	7.0
O00425	Insulin-like growth factor 2 mRNA-binding protein 3	IGF2BP3	2.4.E+05	3.6.E+04	6.7
Q9NTW7	Zinc finger protein 64	ZFP64	1.7.E+06	2.5.E+05	6.6
Q8N3R9	MAGUK p55 subfamily member 5	MPP5	1.3.E+06	2.0.E+05	6.5
Q9UJQ4	Sal-like protein 4	SALL4	1.5.E+07	2.4.E+06	6.0
Q13867	Bleomycin hydrolase	BLMH	4.8.E+05	8.1.E+04	5.9
Q9BUH6	Protein PAXX	PAXX	5.8.E+07	1.0.E+07	5.8
Q99990	Transcription cofactor vestigial-like protein 1	VGLL1	2.5.E+07	4.4.E+06	5.6
P35908	Keratin, type II cytoskeletal 2 epidermal	KRT2	2.5.E+08	4.5.E+07	5.6
Q8N1N4	Keratin, type II cytoskeletal 78	KRT78	1.9.E+06	3.6.E+05	5.2

[a]quantitative values of binding.

keratinocytes derived from low-grade cervical intraepithelial neoplasia) reduced the level of HPV16 *E6*I* mRNA (Fig. 4C). We also tested siRNA knockdown against S100A8, which can form a heterodimer with S100A9 and was shown to bind to the LCR (Table 1), but S100A8 knockdown did not significantly affect *E6*I* mRNA levels in CaSki and HeLa cells (data not shown).

We further verified the effect of S100A9 knockdown on viral oncogene expression by assessing protein levels of E7 and p53 (a surrogate marker for E6 expression). As expected, knockdown of S100A9 or TEAD1 efficiently depleted individual target proteins. Upon S100A9 and/or TEAD1 knockdown, we observed reduced E7 levels in CaSki, HeLa, and

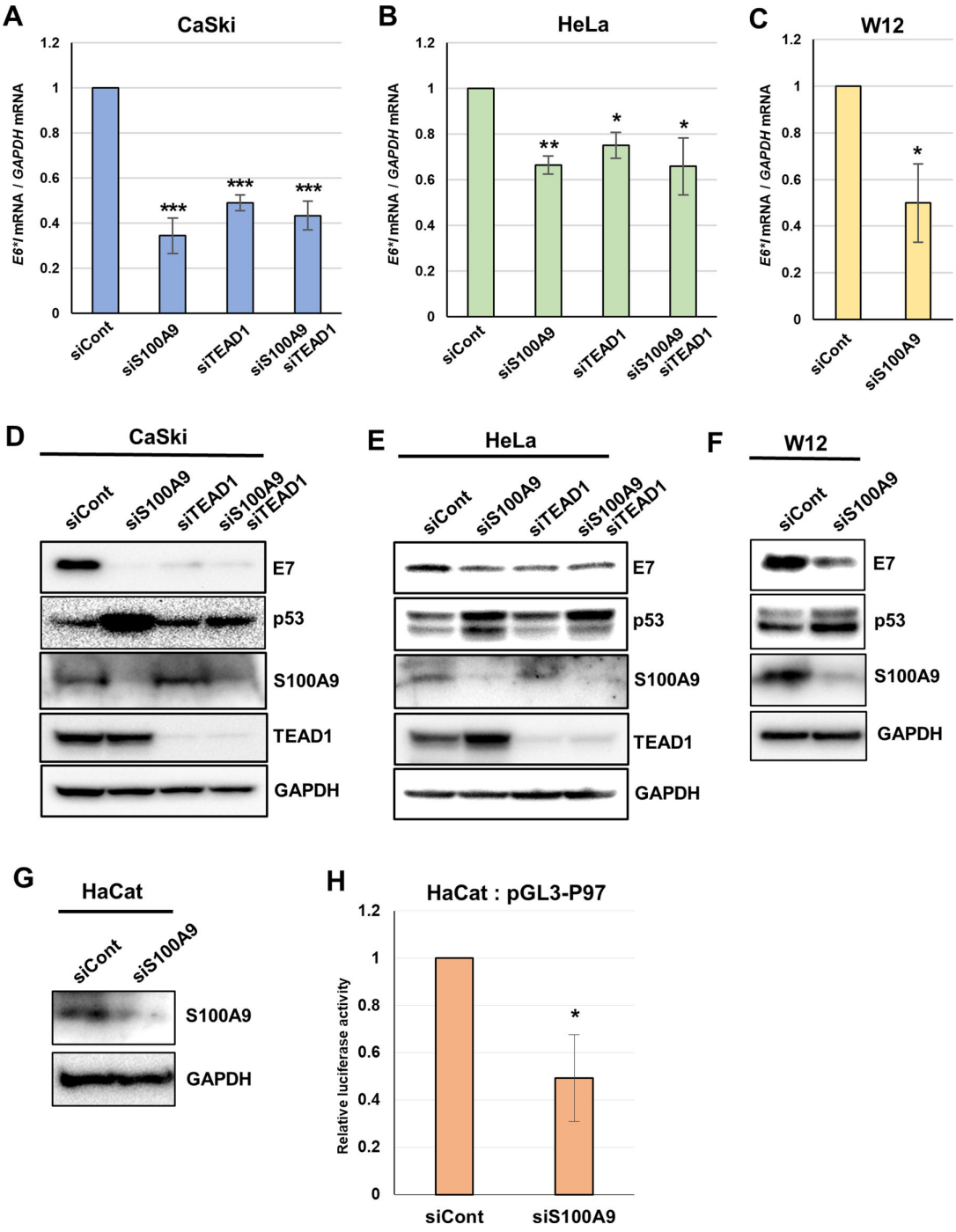

FIG 4 S100A9 contributes to HPV oncogene expression. (A–F) CaSki (A, D), HeLa (B, E), and W12 cells (C, F) were transfected with the indicated siRNAs. Two days after transfection, the levels of HPV16 *E6*I* (A, C) and HPV18 *E6*I* mRNAs (B) were quantified using RT-qPCR and normalized to the levels of glyceraldehyde-3-phosphate dehydrogenase (*GAPDH*) mRNA. HPV16 E7 (D, F) and HPV18 E7 (E) proteins were detected by immunoblotting with the anti-HPV16 and anti-HPV18 E7 antibodies, respectively. p53 protein, which is degraded by E6, was detected using anti-p53 antibodies. The effects of the siRNA were verified by immunoblotting with anti-S100A9 and anti-TEAD1 antibodies. For HeLa and W12 cells, endogenous S100A9 was enriched by immunoprecipitation prior to immunoblotting. GAPDH was used as a loading control. (G) HaCaT cells were transfected with indicated siRNAs, and the effects of the siRNA were verified by immunoblotting with anti-S100A9 antibodies. (H) HaCaT cells were transfected with indicated siRNAs. Six hours later, the cells were transfected with the firefly reporter plasmid (pGL3-P97), together with the Renilla luciferase plasmid. Two days after transfection, the firefly luciferase activity was measured and normalized to the Renilla luciferase activity after background subtraction. The data are averages from three independent experiments, with error bars representing standard deviations. *, $P < 0.05$; **, $P < 0.01$; ***, $P < 0.005$ (Student's *t* test).

W12 cells (Fig. 4D through F), consistent with the mRNA levels in RT-qPCR (Fig. 4A through C). Moreover, we detected increased p53 levels in S100A9-knockdown cells, reflecting reduced E6 levels. Co-transfection of cells with siS100A9 and siTEAD1 did not increase p53 levels because TEAD1 is required for p53 expression (34, 35). Thus, S100A9 knockdown reduces not only mRNA but also protein levels of E6 and E7. We also confirmed that S100A9 knockdown decreased luciferase reporter gene expression driven by the viral P97 promoter (pGL3-P97) in HaCaT cells (Fig. 4G and H). These results indicate that S100A9 enhances HPV oncogene expression via TEAD1 by transactivating the P97 promoter.

Nuclear S100A9 activates HPV oncogene expression

We examined the effects of ectopic S100A9 on HPV oncogene expression by transducing CaSki cells with a retroviral vector encoding S100A9-HA, followed by pooling drug-resistant cells after puromycin selection (CaSki/A9). Immunoblotting analysis detected ectopically expressed S100A9-HA in the cytoplasm but not in the nucleus (Fig. 5A). We observed a modest but significant upregulation in *E6*I* mRNA levels in CaSki/A9 cells compared to those upon transduction with an empty vector (CaSki/MXs) (Fig. 5B). The increased and decreased protein levels of E7 and p53, respectively, were confirmed by immunoblotting (Fig. 5C). We speculated that very low and undetectable levels of S100A9-HA could be present in the nucleus, capable of inducing *E6* and *E7* gene expression.

We further investigated the nuclear functions of S100A9 by fusing nuclear localization signal (NLS) sequences to S100A9-HA (NS100A9-HA) and transducing CaSki cells (CaSki/NA9). We detected both cytoplasmic- and nuclear-localized NS100A9-HA in CaSki/NA9 cells (Fig. 5A). Furthermore, we observed greatly increased *E6*I* mRNA levels in CaSki/NA9 cells (Fig. 5B), with increased E7 and reduced p53 protein levels (Fig. 5C). Ectopic S100A9-HA or NS100A9-HA did not affect TEAD1 levels (Fig. 5A), suggesting that S100A9 is a rate-limiting factor for TEAD1-mediated transcriptional activation.

Next, we examined the effects of ectopic S100A9 on HPV early promoter activity using the luciferase reporter assay. We co-transfected CaSki cells with pGL3-P97 together with pCMV-A9 or an expression plasmid for NS100A9-HA (pCMV-NA9), followed by luciferase activity measurement 2 days after transfection. We found that NS100A9-HA, but not S100A9-HA, significantly activated the P97 promoter (Fig. 5D). Immunoblot analysis revealed S100A9-HA to be exclusively cytoplasmic and NS100A9-HA to be both cytoplasmic and nuclear localized (Fig. 5E). Thus, overexpression of S100A9 alone is sufficient to enhance transcription of HPV oncogenes, with its nuclear localization as a prerequisite for efficient activation.

S100A9 promotes cervical cancer cell growth and reduces their susceptibility to cisplatin

Lastly, we examined whether S100A9 contributes to the growth of cervical cancer cells and their sensitivity to chemotherapy drugs. We transduced CaSki cells with a lentiviral vector expressing short hairpin RNA (shRNA) targeting S100A9 (shS100A9). CaSki cells stably expressing shS100A9 (CaSki/shS100A9) showed reduced levels of *E6*I* mRNA along with *S100A9* mRNA reduction compared to CaSki cells transduced with an empty vector (CaSki/LKO) (Fig. 6A). We found that CaSki/shS100A9 showed reduced cell growth compared to the control cells (Fig. 6B). Furthermore, CaSki/shS100A9 exhibited increased susceptibility to cisplatin, a chemotherapeutic drug for cervical cancer (Fig. 6C). These results are consistent with previous observations that knockdown of S100A9 inhibits proliferation of SiHa cells (an HPV16-positive, cervical cancer cell line) and increases their sensitivity to cisplatin (36, 37).

We further examined whether CaSki/NA9 cells displayed enhanced proliferation and reduced sensitivity to cisplatin. We observed increased proliferation of CaSki/NA9 cells compared to that of the control cells (Fig. 6D). Furthermore, cisplatin treatment revealed significantly increased viability of CaSki/NA9 cells compared to that of the control cells

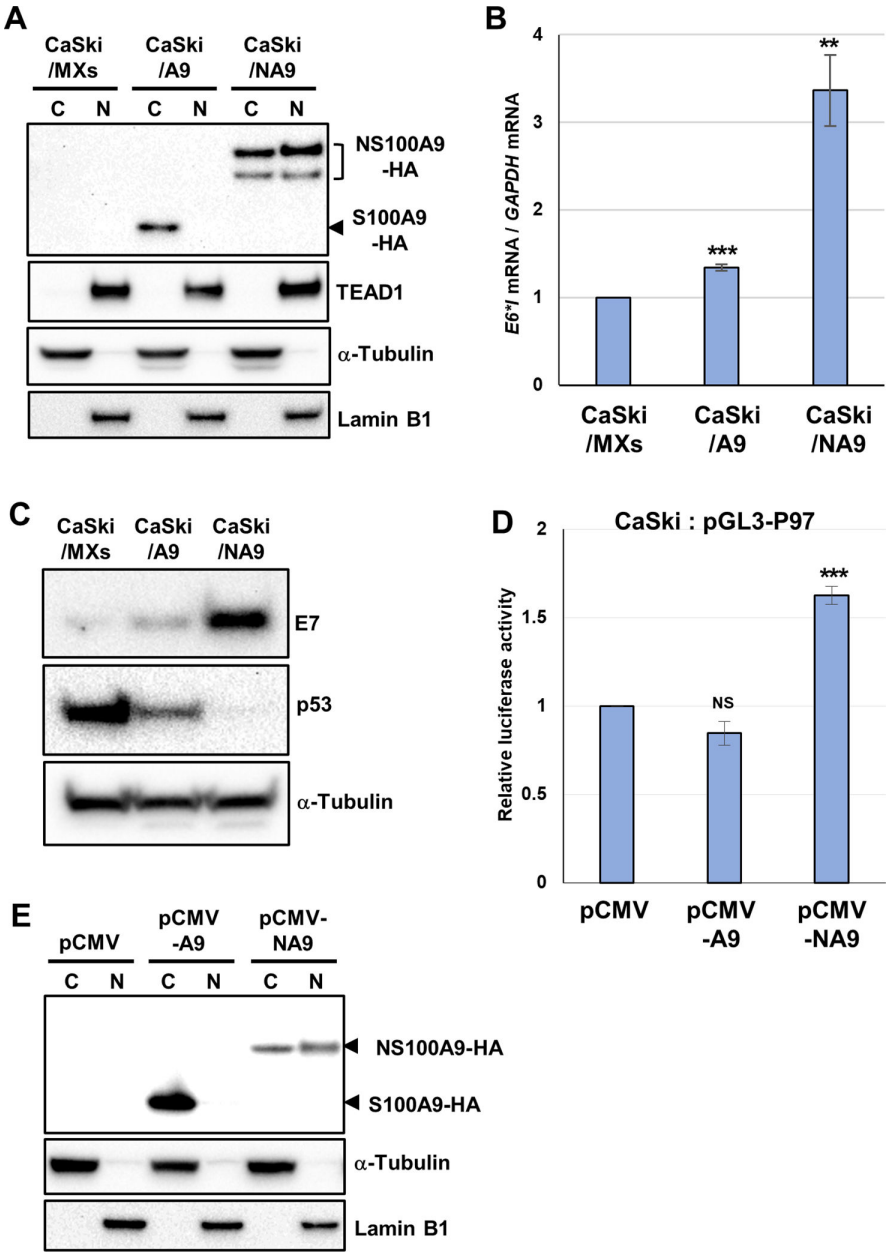

FIG 5 Nuclear S100A9 activates HPV oncogene expression. (A) Cytoplasmic (C) and nuclear (N) fractions of CaSki cells stably expressing S100A9-HA (CaSki/A9), NS100A9-HA (CaSki/NA9), or selection marker alone (CaSki/MXs) were analyzed for expression of S100A9-HA or NS100A9-HA and TEAD1 by immunoblotting with anti-HA and anti-TEAD1 antibodies, respectively. α-Tubulin and lamin B1 were used as cytoplasmic and nuclear markers, respectively. (B) The levels of HPV16 *E6*I* mRNA in CaSki/MXs, CaSki/A9, or CaSki/NA9 were determined by RT-qPCR with normalization to the level of glyceraldehyde-3-phosphate dehydrogenase (*GAPDH*) mRNA. (C) CaSki/MXs, CaSki/A9, or CaSki/NA9 cells were analyzed by immunoblotting using anti-HPV16 E7 and anti-p53 antibodies. α-Tubulin was used as a loading control. (D) CaSki cells were transfected with the indicated expression plasmids, together with the HPV16 LCR reporter plasmid (pGL3-P97) and the Renilla luciferase plasmid. Two days after transfection, the firefly luciferase activity was measured with normalization to the Renilla luciferase activity. The levels of luciferase activity are presented as fold increase compared with that obtained from cells transfected with pGL3-P97 with the empty vector (pCMV). (E) Cytoplasmic (C) and nuclear (N) fractions of CaSki cells transiently transfected with the expression vector for S100A9-HA (pCMV-A9), NS100A9-HA (pCMV-NA9), or the empty vector (pCMV) were analyzed for expression of S100A9-HA or NS100A9-HA by immunoblotting with anti-HA antibodies. α-Tubulin and lamin B1 were used as cytoplasmic and nuclear markers, respectively. The data are averages from three independent experiments, with error bars representing standard deviations. NS, $P > 0.05$; **, $P < 0.005$; ***, $P < 0.001$ (Student's *t* test).

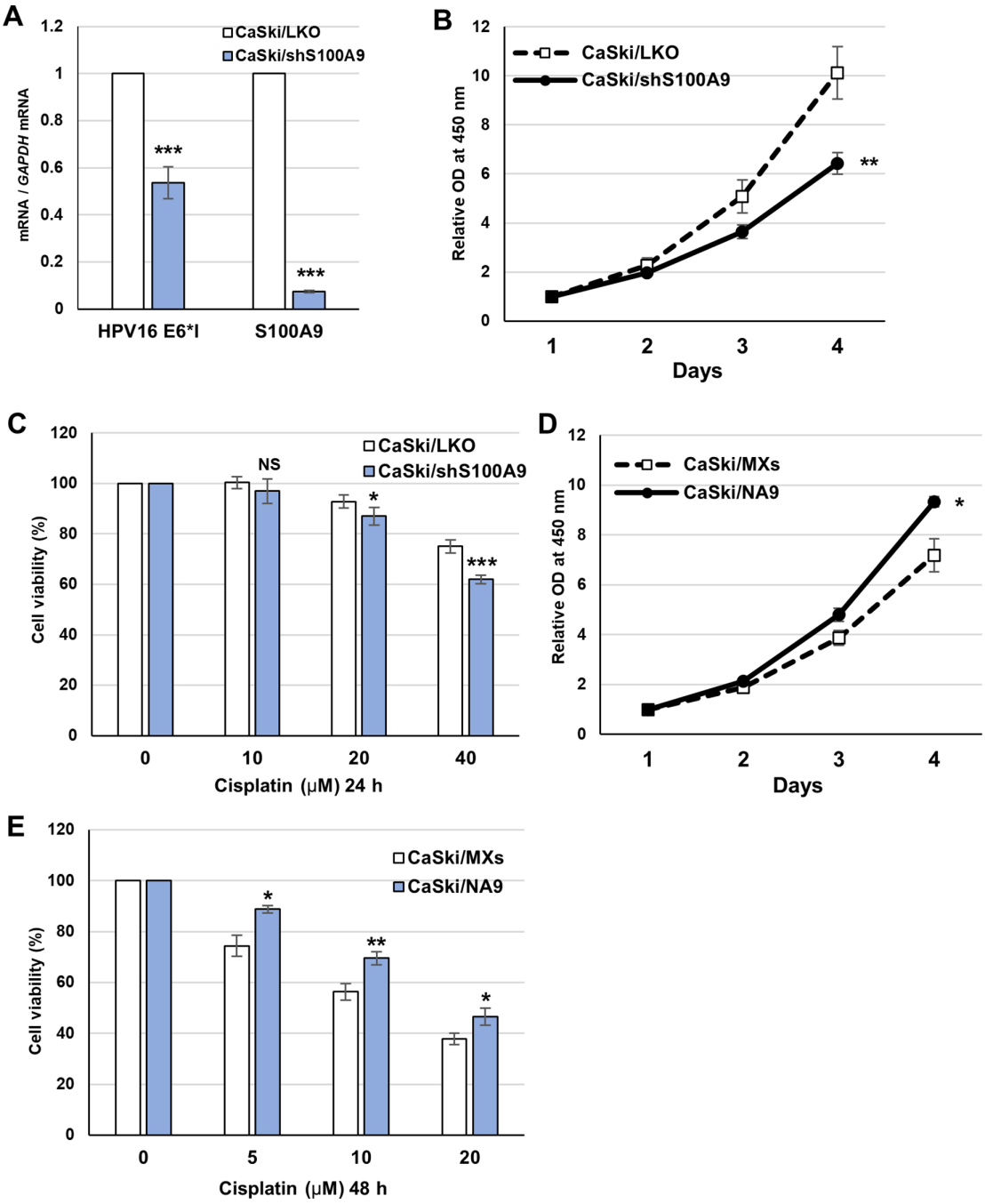

FIG 6 S100A9 promotes cervical cancer cell growth and reduces their sensitivity to cisplatin. (A) CaSki cells stably expressing short hairpin RNA against S100A9 (CaSki/shS100A9) or selection marker alone (CaSki/LKO) were analyzed for expression of HPV16 *E6*I* and *S100A9* mRNAs by RT-qPCR with normalization to the level of glyceraldehyde-3-phosphate dehydrogenase (*GAPDH*) mRNA. The RT-qPCR data are averages from three independent experiments, with error bars representing standard deviations. (B) CaSki/shS100A9 or CaSki/LKO cells were examined for cell viability using the Cell Counting Kit-8 (Dojindo) on the indicated days. (C) CaSki/shS100A9 or CaSki/LKO cells were incubated in the culture medium containing the indicated concentrations of cisplatin for 24 h. Cell viability was measured and presented as a percentage of cell viability of cells incubated with DMSO alone (0 μM). (D) CaSki cells stably expressing NS100A9-HA (CaSki/NA9) or selection marker alone (CaSki/MXs) were examined for cell viability as described above. (E) CaSki/NA9 or CaSki/MXs cells were incubated in the culture medium containing the indicated concentration of cisplatin for 48 h. The cell viability data are the average of relative optical density (OD) values (450 nm) obtained from three wells of a 96-well plate, with error bars representing standard deviations. Representative results are shown from three independent experiments with similar results. NS, $P > 0.05$; *, $P < 0.05$; **, $P < 0.01$; ***, $P < 0.005$ (Student's *t* test).

(Fig. 6E). Thus, nuclear S100A9 promotes the growth of cervical cancer cells and decreases their susceptibility to cisplatin, presumably contributing to a malignant phenotype of cancer cells.

DISCUSSION

Cervical inflammation caused by genital infection with HPV or other pathogenic viruses, bacteria, and fungi contributes to the development of HPV-induced cervical cancer (3–7). However, the molecular mechanisms underlying the relationship between inflammation and cervical carcinogenesis are not fully understood. In this study, we demonstrated that the nuclear proinflammatory cytokine S100A9 activates the transcription of HPV oncogenes via TEAD1. S100A9 is induced by inflammatory stimuli in epithelial cells (19, 21) where HPV gene expression occurs. Our data highlight S100A9 as an important host factor that directly links inflammation to viral carcinogenesis. These results also suggest an ambivalent role for S100A9 in microbial infection as an extracellular and cytoplasmic S100A9 protects against pathogen infections, whereas nuclear S100A9 promotes viral gene expression.

S100A9 is encoded in the epidermal differentiation complex locus on chromosome 1q21, where many genes involved in epidermal differentiation and cornification are clustered (38). This implies that S100A9 functions primarily in epidermal development, differentiation, and homeostasis. In keratinocytes, S100A9 expression is induced by other proinflammatory cytokines, including interleukin (IL)−1, IL-17, IL-22, and tumor necrosis factor α (39–42). Bacterial flagellin also upregulates S100A9 expression via TLR5 (43), and S100A9 is upregulated during epithelial wound healing and keratinocyte differentiation (19, 44). Thus, various exogenous stimuli, including inflammation, infection, wound healing, and cell differentiation, may enhance HPV oncogene expression via S100A9. On the other hand, our preliminary experiments showed that introduction of the HPV16 genome into primary human keratinocytes did not increase S100A9 mRNA levels (data not shown), suggesting that the virus does not autonomously enhance its gene expression through S100A9.

In contrast to its extracellular and cytoplasmic functions, nuclear functions of S100A9 are poorly understood. In myeloid cells, S100A9 induces miRNA expression in association with STAT3 and C/EBPβ during sepsis (26), and in mouse keratinocytes, S100A9 regulates *C3* gene expression by associating with its promoter region (25). Song and Struhl (27) recently reported that S100A9 induces cellular oncogene expression during breast epithelial cell transformation by binding to promoters and enhancers. They also showed that S100A9 forms complexes with AP-1, STAT3, and C/EBPβ and that the binding motifs for these TFs are enriched in S100A9-associated genomic regions. Intriguingly, these TFs are also involved in HPV gene expression (8, 9, 45–47), suggesting that the transcriptional machinery for viral oncogenes shares common molecular bases with cellular oncogenes. As the TEAD family of TFs interacts with AP-1 and STAT3 (48–51), a large multivalent complex of S100A9, TEAD1, AP-1, STAT3, and C/EBPβ may be recruited to the LCR to induce HPV transcription.

The molecular mechanisms by which S100A9 activates viral transcription remain unclear. Ectopic expression of S100A9 alone was sufficient to enhance HPV oncogene expression. Moreover, S100A9 reportedly activated transcription from the *Saccharomyces cerevisiae* GAL4 upstream activator sequence when fused to the GAL4 DNA-binding domain (27). These observations suggest that S100A9 possesses transactivation activity and acts as a transcriptional coactivator. Since S100A9 interacts with multiple TFs and chromatin components, such as histones (25–27), it could facilitate the assembly of TFs on the LCR and activate transcription epigenetically. Interestingly, S100A9 contains an intrinsically disordered region in its C-terminal tail (20), with the potential to cause liquid-liquid phase separation (52), raising the possibility that S100A9 binding to the LCR drives phase separation to generate transcription factories. Our observation that nuclear S100A9 is enriched in the insoluble fraction supports this hypothesis. Further studies are required to elucidate the precise role of S100A9 in activating HPV transcription.

We previously showed that VGLL1 associates with the LCR via TEAD1 and induces HPV gene expression (16). Our Co-IP experiments demonstrated that anti-S100A9 antibodies co-precipitated not only TEAD1 but also VGLL1, suggesting that S100A9 and VGLL1 can simultaneously bind to TEAD1 to regulate transcription. Although TEAD1 is ubiquitously expressed in a variety of tissues (17), S100A9 and VGLL1 display tissue-specific expression, and epithelial cells are one of the few cell types to express both S100A9 and VGLL1 (19, 53, 54). Thus, these cofactors may play crucial roles in determining the tissue specificity of HPV gene expression in collaboration with ubiquitous TFs, such as TEAD1.

The expression of S100A9 is upregulated in various types of tumors of epithelial origin, including cervical cancer (55–59). Since S100A9 is not expressed in undifferentiated primary keratinocytes (40, 43, 60), it may be a novel therapeutic target for cervical cancer and precancer. Indeed, we and others have demonstrated that shRNA-mediated knockdown of S100A9 inhibits growth of cervical cancer cells and sensitizes them to cisplatin (36, 37). We showed that S100A9 directly binds to TEAD1; thus, selective inhibitors that disrupt the S100A9/TEAD1 interaction may be useful for suppressing HPV oncogene expression, warranting further investigation into the three-dimensional structure of the S100A9/TEAD1 complex. Furthermore, immunohistochemical detection of nuclear S100A9 may be a useful prognostic biomarker for progression from cervical precancer to invasive cancer.

MATERIALS AND METHODS

Cell culture

CaSki, HeLa, HaCaT, and HEK293FT (Thermo Fisher Scientific, Waltham, MA, USA) cells were cultured in Dulbecco's modified minimal essential medium (DMEM) supplemented with 10% FBS. W12 (clone 20863) and HCK1T cells were cultured in keratinocyte serum-free medium (Thermo Fisher Scientific) supplemented with 30 µg/mL bovine pituitary extract and 1 ng/mL human recombinant epidermal growth factor.

Plasmids

The expression plasmid for S100A9-HA (pCMV-A9) was constructed by amplifying *S100A9* cDNA from CaSki cell cDNA by PCR using the forward primer 5′-GCG GCC GCC ACC ATG ACT TGC AAA ATG TCG CA-3′ and reverse primer 5′-GGC GGC CGC CTA GGC GTA GTC GGG GAC GTC GTA GGG GTA ACT TCC ACC TCC ACC TCC GGG GGT GCC CTC CCC GAG GC-3′ (the HA tag sequence is underlined), followed by cloning into pCMV, which was created by removing the *β-galactosidase* gene from pCMV-β (TaKaRa Bio, Shiga, Japan). To produce pCMV-NA9, which encodes S100A9 fused to NLSs, a coding sequence for the 3 × NLS (PKKKRKVD) was inserted into both the 5′ and 3′ ends of *S100A9* of pCMV-A9. The expression plasmid for FLAG-TEAD1 (pCMV-FLAG-TEAD1) was generated by inserting the coding sequence for the FLAG tag into the 5′ end of the *TEAD1* gene of pCMV-TEAD1 (32).

DNA-pulldown assay

Nuclei were isolated from CaSki cells using a nuclear extraction kit (Abcam, Cambridge, UK), suspended in buffer A (20 mM Tris-HCl [pH 8.0], 420 mM NaCl, 0.1% NP-40,10% glycerol, cOmplete protease inhibitor [Merck, Darmstadt, Germany], and PhosSTOP [Merck]), and incubated on ice for 1 h. The nuclear suspension was diluted with buffer B (20 mM Tris-HCl [pH 8.0], 0.1% NP-40, 10% glycerol, 0.1% bovine serum albumin, 1 mM DTT, cOmplete protease inhibitor [Merck], and PhosSTOP [Merck]) to a final NaCl concentration of 100 mM. After centrifugation, the supernatant containing soluble nuclear extracts was used for DNA-pulldown assays. Biotinylated DNA probes were prepared by PCR using pGL3-P97 (16) as the WT LCR probe and pGL3-P97/PTm (16) as the Mut LCR probe template. The following primers were used: WT forward, 5′-biotin-GCA ACT ACT GAA TCA CTA TG-3′, Mut forward, 5′-biotin-GCA ACT ACT GAA TCA CGA

CG-3′, and WT/Mut reverse, 5′-AGT TTA AAC CTT ATG CCA AA-3′. Biotinylated WT or Mut LCR probes were coupled to Dynabeads/M-280 streptavidin (Dynal Biotech, Oslo, Norway) as previously described (32). The nuclear extract was then incubated with DNA-coupled magnetic beads and poly(dI-dC) at 4°C for 2 h. The beads were washed three times with buffer C (20 mM Tris-HCl [pH 8.0], 100 mM NaCl, 0.1% NP-40, 10% glycerol, and 1 mM DTT), once with 50 mM Tris-HCl (pH 8.0), and subjected to nano-liquid chromatography coupled with tandem MS.

S100A9-HA and FLAG-TEAD1 were expressed in HEK293FT cells transfected with either pCMV-A9 or pCMV-FLAG-TEAD1. S100A9-HA and FLAG-TEAD1 were then purified using an HA-tagged protein purification kit (MBL, Tokyo, Japan) and a DDDDK-tagged protein purification kit (MBL), respectively, according to the manufacturer's instructions. Purified S100A9-HA and/or FLAG-TEAD1 were incubated with the WT or Mut LCR probe conjugated to beads in buffer C containing protease inhibitors. After washing the beads, the bound proteins were eluted by boiling the beads in sodium dodecyl sulfate (SDS) sample buffer, followed by protein analysis by immunoblotting.

DIA-MS analysis

DIA-MS analyses were performed by Kazusa Genome Technologies (Chiba, Japan). Briefly, the proteins bound to the beads were digested with trypsin, reduced with DTT, and alkylated with iodoacetamide. The peptides were dried after acidification with 5% trifluoroacetic acid and dissolved in 3% acetonitrile and 0.1% formic acid. MS data were obtained using an UltiMate 3000 RSLC nanoLC system (Thermo Fisher Scientific) and analyzed using Scaffold DIA (Proteome Software, Portland, OR, USA). The protein identification threshold was a peptide or protein false discovery rate below 1%.

Immunofluorescence microscopy

CaSki and HeLa cells were fixed with 4% paraformaldehyde in phosphate-buffered saline (PBS) and permeabilized with 0.2% Triton X-100 in PBS. After blocking with PBS containing 5% goat serum, the cells were incubated with anti-S100A9 antibodies (11145-R018, Sino Biological, Beijing, China), followed by incubation with Alexa Fluor 546-conjugated anti-rabbit IgG antibodies (Thermo Fisher Scientific). The cells were mounted using ProLong Gold antifade mounting medium with DAPI (Thermo Fisher Scientific) and examined under a confocal microscope (FluoView1000, OLYMPUS, Tokyo, Japan).

TPA treatment

TPA was purchased from FUJIFILM Wako Pure Chemical (Osaka, Japan) and was dissolved in DMSO. CaSki cells were cultured for 24 h in DMEM supplemented with 0.5% FBS before TPA treatment. TPA was added to the culture medium for 4 h at a final concentration of 200 ng/mL.

Cell fractionation

Cells were divided into cytoplasmic protein fractions and nuclear pellets using a nuclear extraction kit (Abcam). The nuclear pellet was dissolved in buffer D (50 mM Tris-HCl [pH 6.8], 100 mM NaCl, 8 M urea, 2% SDS, 10% glycerol, 5% 2-mercaptoethanol, and bromophenol blue) to obtain a nuclear protein fraction. To obtain soluble and insoluble nuclear protein fractions, the nuclear pellet was suspended in buffer E (50 mM Tris-HCl [pH 8.0], 420 mM NaCl, 1 mM MgCl2, 0.1% NP-40,10% glycerol, cOmplete protease inhibitor [Merck], and PhosSTOP [Merck]) and incubated on ice for 1 h. After centrifugation, the supernatant was collected as the soluble nuclear protein fraction, and the pellet was dissolved in buffer D as the insoluble nuclear protein fraction.

Immunoblotting

Immunoblotting was performed as previously described (32). The primary antibodies used were as follows: anti-HA tag (12013819001; Merck), anti-TEAD1 (610922; BD Transduction Laboratories, San Diego, CA, USA), anti-TEAD4 (sc-101184; Santa Cruz Biotechnology, Dallas, TX, USA), anti-VGLL1 (a mixture of clones HPA042403 and HPA064616; Merck), anti-S100A9 (26992–1-AP; Proteintech, Rosemont, IL, USA), anti-Ku70 (GTX101820; GeneTex, Irvine, CA, USA), anti-HPV16 E7 (a mixture of #28–0006 [Thermo Fisher Scientific] and sc-6981 [Santa Cruz Biotechnology]), anti-HPV18 E7 (ab100953; Abcam, Cambridge, UK), anti-p53 (sc-126; Santa Cruz Biotechnology), anti-glyceraldehyde-3-phosphate dehydrogenase (GAPDH; 015–25473; FUJIFILM Wako Pure Chemical), anti-α-Tubulin (sc-32293; Santa Cruz Biotechnology), anti-Lamin B1 (sc-6216; Santa Cruz Biotechnology), and anti-c-Fos (sc-52; Santa Cruz Biotechnology) antibodies. For HeLa, W12, and HaCat cells, endogenous S100A9 was enriched by immunoprecipitation prior to immunoblotting.

Co-IP experiment

Nuclei were isolated from CaSki cells as described above, suspended in buffer E, and incubated on ice for 1 h. The nuclear suspension was diluted with buffer F (50 mM Tris-HCl [pH 8.0], 1 mM MgCl2, 0.1% NP-40, 10% glycerol, cOmplete protease inhibitor [Merck], and PhosSTOP [Merck]) to a final concentration of 100 mM NaCl and incubated with benzonase (50 U/mL; Merck) for 1.5 h at room temperature. After centrifugation, the supernatant was incubated with antibodies at 4°C overnight. The lysate was further incubated with 5 µL of Sera-Mag SpeedBeads Protein A/G Magnetic Particles (Cytiva, Marlborough, MA, USA) at 4°C for 2 h. The beads were washed three times with buffer G (50 mM Tris-HCl [pH 8.0], 100 mM NaCl, 0.1% NP-40, and 10% glycerol), and the bound proteins were eluted in SDS sample buffer. The recovered proteins were analyzed by immunoblotting.

When Co-IP experiments were performed with *in vitro*-translated proteins, proteins were synthesized using PURERex 2.0 (GeneFrontier, Chiba, Japan), according to the manufacturer's instructions. Briefly, DNA fragments encoding S100A9-HA or FLAG-TEAD1 were obtained by PCR from pCMV-A9 or pCMV-FLAG-TEAD1, respectively, and incubated with *in vitro* translation solutions at 37°C for 6 h. The reaction mixture was diluted with an equal volume of H_2O, and after centrifugation, the supernatant containing soluble proteins was used for the Co-IP experiments. The proteins were incubated with antibodies in buffer G containing benzonase (50 U/mL, Merck) at 4°C for 1 h, and bound proteins were recovered and analyzed as described above. Antibodies used for immunoprecipitation were anti-TEAD1 (P28347; Cusabio, Houston, TX, USA), anti-S100A9 (11145-R018; Sino Biological), and normal rabbit IgG (sc-2027; Santa Cruz Biotechnology) antibodies.

ChIP assay

CaSki and HeLa cells were fixed with ChIP Cross-link Gold (Diagenode, Liege, Belgium) to cross-link protein-protein interactions, followed by fixation with formaldehyde for DNA-protein cross-linking. ChIP assays were performed using SimpleChIP Plus enzymatic chromatin immunoprecipitation kits (Cell Signaling Technology, Beverly, MA, USA), according to the manufacturer's instructions, with the exception that Sera-Mag SpeedBeads Protein A/G Magnetic Particles (Cytiva, Marlborough, MA, USA) were used to capture antibodies. The antibodies used for immunoprecipitation were anti-S100A9 (GTX129575; GeneTex) and normal rabbit IgG (2729S; Cell Signaling Technology) antibodies. Precipitated HPV16 or HPV18 LCR DNA fragments and the promoter region of the *C3* and *APOBEC3B* genes were quantified using real-time PCR. The nucleotide sequences of the primers for the HPV16 and HPV18 LCRs and the *APOBEC3B* gene were described previously (16, 32). The following primers were used for the *C3* gene: forward, 5′- GGT TGT CAA ACC ACA GTG CC -3′and reverse, 5′- TCT CCC AAT TGC CCC ATT CC -3′.

siRNA transfection

Cells were transfected with siRNA using the Lipofectamine RNAiMAX transfection reagent (Thermo Fisher Scientific). The following siRNAs were purchased from Horizon Discovery (Cambridge, UK): non-targeting control (catalog number: D-001206–13), *S100A9* (catalog number: M-011384–02), and *TEAD1* (catalog number: L-012603–00).

RT-qPCR

The levels of HPV16 *E6*I* and HPV18 *E6*I* mRNAs were determined by RT-qPCR, as previously described (16). The amount of cDNA of the target genes was normalized to the amount of concurrently amplified *GAPDH* mRNA. The nucleotide sequences of the primers were described previously (16, 61).

Luciferase reporter assay

Cells were transfected with pGL3-P97 (16), either alone or in combination with expression plasmids, together with phRG-TK (Promega, Madison, WI, USA), which express Renilla luciferase. When cells were co-transfected with siRNAs and plasmid DNAs, they were transfected with siRNA 6 h before plasmid transfection. Firefly and Renilla luciferase activities were measured 2 days post-transfection using a Dual-Glo luciferase assay system (Promega) on an Arvo MX luminescence counter (PerkinElmer, Waltham, MA, USA). The firefly luciferase activity was normalized to the Renilla luciferase activity after subtraction of the background activity from untransfected cells.

Lentiviral and retroviral transduction

CaSki cells stably expressing shS100A9 were produced by transduction with lentiviral vectors, as previously described (16). The vector plasmid encoding shS100A9 was purchased from Merck (TRCN0000425882). CaSki cells stably expressing S100A9-HA or NS100A9-HA were produced by transduction with retroviral vectors, as previously described (32). The transduced cells were selected by treatment with 2 µg/mL puromycin, and the surviving cells were pooled and used for downstream experiments.

Cell viability assay

Cells were seeded at 1×10^3 cells/well in 96-well plates. Viable cells were counted using a Cell Counting Kit-8 (Dojindo, Kumamoto, Japan) at the indicated time points. Cisplatin sensitivity was determined by plating cells (2×10^3 cells/well) in a 96-well plate followed by incubation in culture medium containing cisplatin (Adipogen, San Diego, CA, USA) or DMSO alone for 24 or 48 h and cell viability measurement.

ACKNOWLEDGMENTS

We thank Tohru Kiyono for providing us with HCK1T cells.

This work was supported by a Grant-in-Aid for Scientific Research from the Japan Society for the Promotion of Science (grant numbers JP18K09244 and JP21K09461) awarded to S.M.

AUTHOR AFFILIATION

[1]Pathogen Genomics Center, National Institute of Infectious Diseases, Tokyo, Japan

AUTHOR ORCIDs

Seiichiro Mori http://orcid.org/0009-0003-7928-2900

FUNDING

Funder	Grant(s)	Author(s)
MEXT | Japan Society for the Promotion of Science (JSPS)	JP18K09244, JP21K09461	Seiichiro Mori

AUTHOR CONTRIBUTIONS

Seiichiro Mori, Conceptualization, Data curation, Formal analysis, Funding acquisition, Investigation, Methodology, Project administration, Resources, Software, Supervision, Validation, Visualization, Writing – original draft | Yoshiyuki Ishii, Methodology, Resources, Writing – review and editing | Takamasa Takeuchi, Methodology, Resources, Writing – review and editing | Iwao Kukimoto, Methodology, Resources, Writing – review and editing

REFERENCES

1. Doorbar J, Egawa N, Griffin H, Kranjec C, Murakami I. 2015. Human papillomavirus molecular biology and disease association. Rev Med Virol 25 Suppl 1:2–23. https://doi.org/10.1002/rmv.1822
2. Longworth MS, Laimins LA. 2004. Pathogenesis of human papillomaviruses in differentiating epithelia. Microbiol Mol Biol Rev 68:362–372. https://doi.org/10.1128/MMBR.68.2.362-372.2004
3. Boccardo E, Lepique AP, Villa LL. 2010. The role of inflammation in HPV carcinogenesis. Carcinogenesis 31:1905–1912. https://doi.org/10.1093/carcin/bgq176
4. Hemmat N, Bannazadeh Baghi H. 2019. Association of human papillomavirus infection and inflammation in cervical cancer. Pathog Dis 77:ftz048. https://doi.org/10.1093/femspd/ftz048
5. Zhou ZW, Long HZ, Cheng Y, Luo HY, Wen DD, Gao LC. 2021. From microbiome to inflammation: the key drivers of cervical cancer. Front Microbiol 12:767931. https://doi.org/10.3389/fmicb.2021.767931
6. Ntuli L, Mtshali A, Mzobe G, Liebenberg LJ, Ngcapu S. 2022. Role of immunity and vaginal microbiome in clearance and persistence of human papillomavirus infection. Front Cell Infect Microbiol 12:927131. https://doi.org/10.3389/fcimb.2022.927131
7. Molina MA, Coenen BA, Leenders WPJ, Andralojc KM, Huynen MA, Melchers WJG. 2022. Assessing the cervicovaginal microbiota in the context of hrHPV infections: temporal dynamics and therapeutic strategies. mBio 13:e0161922. https://doi.org/10.1128/mbio.01619-22
8. Kajitani N, Satsuka A, Kawate A, Sakai H. 2012. Productive lifecycle of human papillomaviruses that depends upon squamous epithelial differentiation. Front Microbiol 3:152. https://doi.org/10.3389/fmicb.2012.00152
9. Bernard HU. 2013. Regulatory elements in the viral genome. Virology 445:197–204. https://doi.org/10.1016/j.virol.2013.04.035
10. Chong T, Apt D, Gloss B, Isa M, Bernard HU. 1991. The enhancer of human papillomavirus type 16: binding sites for the ubiquitous transcription factors Oct-1, NFA, TEF-2, Nf1, and AP-1 participate in epithelial cell-specific transcription. J Virol 65:5933–5943. https://doi.org/10.1128/JVI.65.11.5933-5943.1991
11. Gloss B, Yeo-Gloss M, Meisterenst M, Rogge L, Winnacker EL, Bernard HU. 1989. Clusters of nuclear factor I binding sites identify enhancers of several papillomaviruses but alone are not sufficient for enhancer function. Nucleic Acids Res 17:3519–3533. https://doi.org/10.1093/nar/17.9.3519
12. Chong T, Chan WK, Bernard HU. 1990. Transcriptional activation of human papillomavirus 16 by nuclear factor I, Ap1, steroid receptors and a possibly novel transcription factor, PVF: a model for the composition of genital papillomavirus enhancers. Nucleic Acids Res 18:465–470. https://doi.org/10.1093/nar/18.3.465
13. Thierry F, Spyrou G, Yaniv M, Howley P. 1992. Two Ap1 sites binding JunB are essential for human papillomavirus type 18 transcription in keratinocytes. J Virol 66:3740–3748. https://doi.org/10.1128/JVI.66.6.3740-3748.1992
14. Ishiji T, Lace MJ, Parkkinen S, Anderson RD, Haugen TH, Cripe TP, Xiao JH, Davidson I, Chambon P, Turek LP. 1992. Transcriptional enhancer factor (TEF)-1 and its cell-specific co-activator activate human papillomavirus-16 E6 and E7 oncogene transcription in keratinocytes and cervical carcinoma cells. EMBO J 11:2271–2281. https://doi.org/10.1002/j.1460-2075.1992.tb05286.x
15. Warburton A, Redmond CJ, Dooley KE, Fu H, Gillison ML, Akagi K, Symer DE, Aladjem MI, McBride AA, Ott M. 2018. HPV integration hijacks and multimerizes a cellular enhancer to generate a viral-cellular super-enhancer that drives high viral oncogene expression. PLoS Genet 14:e1007179. https://doi.org/10.1371/journal.pgen.1007179
16. Mori S, Takeuchi T, Ishii Y, Kukimoto I. 2020. The transcriptional Cofactor VGLL1 drives transcription of human papillomavirus early genes via TEAD1. J Virol 94:e01945-19. https://doi.org/10.1128/JVI.01945-19
17. Pobbati AV, Hong W. 2013. Emerging roles of TEAD transcription factors and its coactivators in cancers. Cancer Biol Ther 14:390–398. https://doi.org/10.4161/cbt.23788
18. Maeda T, Chapman DL, Stewart AFR. 2002. Mammalian vestigial-like 2, a cofactor of TEF-1 and MEF2 transcription factors that promotes skeletal muscle differentiation. J Biol Chem 277:48889–48898. https://doi.org/10.1074/jbc.M206858200
19. Kerkhoff C, Voss A, Scholzen TE, Averill MM, Zänker KS, Bornfeldt KE. 2012. Novel insights into the role of S100A8/A9 in skin biology. Exp Dermatol 21:822–826. https://doi.org/10.1111/j.1600-0625.2012.01571.x
20. Markowitz J, Carson WE. 2013. Review of S100A9 biology and its role in cancer. Biochim Biophys Acta 1835:100–109. https://doi.org/10.1016/j.bbcan.2012.10.003
21. Wang S, Song R, Wang Z, Jing Z, Wang S, Ma J. 2018. S100A8/A9 in inflammation. Front Immunol 9:1298. https://doi.org/10.3389/fimmu.2018.01298
22. Vogl T, Tenbrock K, Ludwig S, Leukert N, Ehrhardt C, van Zoelen MAD, Nacken W, Foell D, van der Poll T, Sorg C, Roth J. 2007. Mrp8 and Mrp14 are endogenous activators of toll-like receptor 4, promoting lethal, endotoxin-induced shock. Nat Med 13:1042–1049. https://doi.org/10.1038/nm1638
23. Hermani A, De Servi B, Medunjanin S, Tessier PA, Mayer D. 2006. S100A8 and S100A9 activate MAP kinase and NF-kappaB signaling pathways and trigger translocation of RAGE in human prostate cancer cells. Exp Cell Res 312:184–197. https://doi.org/10.1016/j.yexcr.2005.10.013
24. Damo SM, Kehl-Fie TE, Sugitani N, Holt ME, Rathi S, Murphy WJ, Zhang Y, Betz C, Hench L, Fritz G, Skaar EP, Chazin WJ. 2013. Molecular basis for manganese sequestration by calprotectin and roles in the innate immune response to invading bacterial pathogens. Proc Natl Acad Sci U S A 110:3841–3846. https://doi.org/10.1073/pnas.1220341110
25. Schonthaler HB, Guinea-Viniegra J, Wculek SK, Ruppen I, Ximénez-Embún P, Guío-Carrión A, Navarro R, Hogg N, Ashman K, Wagner EF. 2013. S100A8-S100A9 protein complex mediates psoriasis by regulating the expression of complement factor C3. Immunity 39:1171–1181. https://doi.org/10.1016/j.immuni.2013.11.011
26. Alkhateeb T, Kumbhare A, Bah I, Youssef D, Yao ZQ, McCall CE, El Gazzar M. 2019. S100A9 maintains myeloid-derived Suppressor cells in chronic sepsis by inducing miR-21 and miR-181B. Mol Immunol 112:72–81. https://doi.org/10.1016/j.molimm.2019.04.019

27. Song R, Struhl K. 2021. S100A8/S100A9 cytokine acts as a transcriptional coactivator during breast cellular transformation. Sci Adv 7:eabe5357. https://doi.org/10.1126/sciadv.abe5357
28. Kawashima Y, Watanabe E, Umeyama T, Nakajima D, Hattori M, Honda K, Ohara O. 2019. Optimization of data-independent acquisition mass spectrometry for deep and highly sensitive proteomic analysis. Int J Mol Sci 20:5932. https://doi.org/10.3390/ijms20235932
29. Uhlén M, Fagerberg L, Hallström BM, Lindskog C, Oksvold P, Mardinoglu A, Sivertsson Å, Kampf C, Sjöstedt E, Asplund A, Olsson I, Edlund K, Lundberg E, Navani S, Szigyarto C-K, Odeberg J, Djureinovic D, Takanen JO, Hober S, Alm T, Edqvist P-H, Berling H, Tegel H, Mulder J, Rockberg J, Nilsson P, Schwenk JM, Hamsten M, von Feilitzen K, Forsberg M, Persson L, Johansson F, Zwahlen M, von Heijne G, Nielsen J, Pontén F. 2015. Tissue-based map of the human proteome. Science 347:1260419. https://doi.org/10.1126/science.1260419
30. Narisawa-Saito M, Handa K, Yugawa T, Ohno S, Fujita M, Kiyono T. 2007. HPV16 E6-mediated stabilization of ErbB2 in neoplastic transformation of human cervical keratinocytes. Oncogene 26:2988–2996. https://doi.org/10.1038/sj.onc.1210118
31. Shimizu Y, Inoue A, Tomari Y, Suzuki T, Yokogawa T, Nishikawa K, Ueda T. 2001. Cell-free translation reconstituted with purified components. Nat Biotechnol 19:751–755. https://doi.org/10.1038/90802
32. Mori S, Takeuchi T, Ishii Y, Yugawa T, Kiyono T, Nishina H, Kukimoto I. 2017. Human papillomavirus 16 E6 upregulates APOBEC3B via the TEAD transcription factor. J Virol 91:e02413-16. https://doi.org/10.1128/JVI.02413-16
33. Olmedo-Nieva L, Muñoz-Bello JO, Contreras-Paredes A, Lizano M. 2018. The role of E6 spliced Isoforms (E6*) in human papillomavirus-induced carcinogenesis. Viruses 10:45. https://doi.org/10.3390/v10010045
34. Bai N, Zhang C, Liang N, Zhang Z, Chang A, Yin J, Li Z, Luo N, Tan X, Luo N, Luo Y, Xiang R, Li X, Reisfeld RA, Stupack D, Lv D, Liu C. 2013. Yes-associated protein (YAP) increases chemosensitivity of hepatocellular carcinoma cells by modulation of p53. Cancer Biol Ther 14:511–520. https://doi.org/10.4161/cbt.24345
35. Huang P-Y, Shih I-A, Liao Y-C, You H-L, Lee M-J. 2022. A novel HDAC11 inhibitor potentiates the tumoricidal effects of cordycepin against malignant peripheral nerve sheath tumor through the hippo signaling pathway. Am J Cancer Res 12:873–892.
36. Zhao C, Lu E, Hu X, Cheng H, Zhang J-A, Zhu X. 2018. S100A9 regulates cisplatin chemosensitivity of squamous cervical cancer cells and related mechanism. Cancer Manag Res 10:3753–3764. https://doi.org/10.2147/CMAR.S168276
37. Zha H, Li X, Sun H, Duan L, Yuan S, Li H, Li A, Gu Y, Zhao J, Xie J, Zhou L. 2019. S100A9 promotes the proliferation and migration of cervical cancer cells by inducing epithelial-mesenchymal transition and activating the WNT/β-catenin pathway. Int J Oncol 55:35–44. https://doi.org/10.3892/ijo.2019.4793
38. Mischke D, Korge BP, Marenholz I, Volz A, Ziegler A. 1996. Genes encoding structural proteins of epidermal cornification and S100 calcium-binding proteins form a gene complex ("epidermal differentiation complex") on human chromosome 1q21. J Invest Dermatol 106:989–992. https://doi.org/10.1111/1523-1747.ep12338501
39. Bando M, Hiroshima Y, Kataoka M, Shinohara Y, Herzberg MC, Ross KF, Nagata T, Kido J. 2007. Interleukin-1Alpha regulates antimicrobial peptide expression in human keratinocytes. Immunol Cell Biol 85:532–537. https://doi.org/10.1038/sj.icb.7100078
40. Boniface K, Bernard FX, Garcia M, Gurney AL, Lecron JC, Morel F. 2005. IL-22 inhibits epidermal differentiation and induces proinflammatory gene expression and migration of human keratinocytes. J Immunol 174:3695–3702. https://doi.org/10.4049/jimmunol.174.6.3695
41. Liang SC, Tan XY, Luxenberg DP, Karim R, Dunussi-Joannopoulos K, Collins M, Fouser LA. 2006. Interleukin (IL)-22 and IL-17 are coexpressed by Th17 cells and cooperatively enhance expression of antimicrobial peptides. J Exp Med 203:2271–2279. https://doi.org/10.1084/jem.20061308
42. Guilloteau K, Paris I, Pedretti N, Boniface K, Juchaux F, Huguier V, Guillet G, Bernard FX, Lecron JC, Morel F. 2010. Skin inflammation induced by the synergistic action of IL-17A, IL-22, Oncostatin M, IL-1{Alpha}, and TNF-{Alpha} Recapitulates some features of psoriasis. J Immunol 184:5263–5270. https://doi.org/10.4049/jimmunol.0902464
43. Abtin A, Eckhart L, Gläser R, Gmeiner R, Mildner M, Tschachler E. 2010. The antimicrobial heterodimer S100A8/S100A9 (calprotectin) is upregulated by bacterial flagellin in human epidermal keratinocytes. J Invest Dermatol 130:2423–2430. https://doi.org/10.1038/jid.2010.158
44. Thorey IS, Roth J, Regenbogen J, Halle JP, Bittner M, Vogl T, Kaesler S, Bugnon P, Reitmaier B, Durka S, Graf A, Wöckner M, Rieger N, Konstantinow A, Wolf E, Goppelt A, Werner S. 2001. The Ca2+-binding proteins S100A8 and S100A9 are encoded by novel injury-regulated genes. J Biol Chem 276:35818–35825. https://doi.org/10.1074/jbc.M104871200
45. Struyk L, van der Meijden E, Minnaar R, Fontaine V, Meijer I, ter Schegget J. 2000. Transcriptional regulation of human Papillomavirus type 16 LCR by different C/Ebpbeta Isoforms. Mol Carcinog 28:42–50. https://doi.org/10.1002/(SICI)1098-2744(200005)28:1<42::AID-MC6>3.0.CO;2-8
46. Johannsen E, Lambert PF. 2013. Epigenetics of human papillomaviruses. Virology 445:205–212. https://doi.org/10.1016/j.virol.2013.07.016
47. Morgan EL, Wasson CW, Hanson L, Kealy D, Pentland I, McGuire V, Scarpini C, Coleman N, Arthur JSC, Parish JL, Roberts S, Macdonald A. 2018. STAT3 activation by E6 is essential for the differentiation-dependent HPV18 life cycle. PLoS Pathog 14:e1006975. https://doi.org/10.1371/journal.ppat.1006975
48. Zanconato F, Forcato M, Battilana G, Azzolin L, Quaranta E, Bodega B, Rosato A, Bicciato S, Cordenonsi M, Piccolo S. 2015. Genome-wide association between YAP/TAZ/TEAD and AP-1 at enhancers drives oncogenic growth. Nat Cell Biol 17:1218–1227. https://doi.org/10.1038/ncb3216
49. Liu X, Li H, Rajurkar M, Li Q, Cotton JL, Ou J, Zhu LJ, Goel HL, Mercurio AM, Park JS, Davis RJ, Mao J. 2016. Tead and AP1 coordinate transcription and motility. Cell Rep 14:1169–1180. https://doi.org/10.1016/j.celrep.2015.12.104
50. Feldker N, Ferrazzi F, Schuhwerk H, Widholz SA, Guenther K, Frisch I, Jakob K, Kleemann J, Riegel D, Bönisch U, Lukassen S, Eccles RL, Schmidl C, Stemmler MP, Brabletz T, Brabletz S. 2020. Genome-wide cooperation of EMT transcription factor ZEB1 with YAP and AP-1 in breast cancer. EMBO J 39:e103209. https://doi.org/10.15252/embj.2019103209
51. He L, Pratt H, Gao M, Wei F, Weng Z, Struhl K. 2021. YAP and TAZ are transcriptional co-activators of AP-1 proteins and STAT3 during breast cellular transformation. Elife 10:e67312. https://doi.org/10.7554/eLife.67312
52. Borcherds W, Bremer A, Borgia MB, Mittag T. 2021. How do intrinsically disordered protein regions encode a driving force for liquid-liquid phase separation? Curr Opin Struct Biol 67:41–50. https://doi.org/10.1016/j.sbi.2020.09.004
53. Vaudin P, Delanoue R, Davidson I, Silber J, Zider A. 1999. TONDU (TDU), a novel human protein related to the product of vestigial (Vg) gene of Drosophila melanogaster interacts with vertebrate TEF factors and substitutes for Vg function in wing formation. Development 126:4807–4816. https://doi.org/10.1242/dev.126.21.4807
54. Faucheux C, Naye F, Tréguer K, Fédou S, Thiébaud P, Théze N. 2010. Vestigial like gene family expression in Xenopus: common and divergent features with other vertebrates. Int J Dev Biol 54:1375–1382. https://doi.org/10.1387/ijdb.103080cf
55. Chao A, Wang TH, Lee YS, Hsueh S, Chao AS, Chang TC, Kung WH, Huang SL, Chao FY, Wei ML, Lai CH. 2006. Molecular characterization of adenocarcinoma and squamous carcinoma of the uterine cervix using microarray analysis of gene expression. Int J Cancer 119:91–98. https://doi.org/10.1002/ijc.21813
56. Zhu X, Lv J, Yu L, Zhu X, Wu J, Zou S, Jiang S. 2009. Proteomic identification of differentially-expressed proteins in squamous cervical cancer. Gynecol Oncol 112:248–256. https://doi.org/10.1016/j.ygyno.2008.09.045
57. Zhu X, Jin L, Zou S, Shen Q, Jiang W, Lin W, Zhu X. 2013. Immunohistochemical expression of RAGE and its ligand (S100A9) in cervical lesions. Cell Biochem Biophys 66:843–850. https://doi.org/10.1007/s12013-013-9515-x
58. Chen H, Xu C, Jin Q, Liu Z. 2014. S100 protein family in human cancer. Am J Cancer Res 4:89–115.
59. Zhao Q, He Y, Wang XL, Zhang YX, Wu YM. 2015. Differentially expressed proteins among normal cervix, cervical intraepithelial neoplasia and cervical squamous cell carcinoma. Clin Transl Oncol 17:620–631. https://doi.org/10.1007/s12094-015-1287-x

60. Martinsson H, Yhr M, Enerbäck C. 2005. Expression patterns of S100A7 (psoriasin) and S100A9 (calgranulin-B) in keratinocyte differentiation. Exp Dermatol 14:161–168. https://doi.org/10.1111/j.0906-6705.2005.00239.x

61. Pauklin S, Sernández IV, Bachmann G, Ramiro AR, Petersen-Mahrt SK. 2009. Estrogen directly activates AID transcription and function. J Exp Med 206:99–111. https://doi.org/10.1084/jem.20080521